International Journal of Basic and Applied Sciences, 10 (1) (2021) 1-6

International Journal of Basic and Applied Sciences

Website: www.sciencepubco.com/index.php/IJBAS

Research paper

Corrosion behavior of borate modified Hench's bioglasses containing dopant cobalt oxide

Y. Abdou [1], A. M. Abdelghany [2] *, A. El-gendy [1, 3], F. A. El-Husseiny [1]

[1] *Physics Department, Faculty of Science, Tanta University, Tanta, Egypt*
[2] *Spectroscopy Department, Physics Division, National Research Centre, 33 Elbehouth St., Dokki, Giza,*
[3] *Basic and Applied Science Department, Horus University, International Coastal Rd, New Damietta, Kafr Saad, 34511, Damietta Gov-ernorate, Egypt*
**Corresponding author E-mail: a.m_abdelghany@yahoo.com*

Abstract

Cobalt doped modified borophosphate glasses similar to Hench's bioglass were successfully synthesized using gradually increasing cobalt ions in addition to another sample of Co free glass. Synthesized samples were studied for their bioactivity through immersion in phosphate solution for different time intervals. FTIR absorption spectral data were collected before and after immersion for a prolonged time intervals. Spectral data reveals appearance of absorption band at 573 cm-1 Splitted into 565 cm-1 and 603 cm-1 after one week of immersion supporting the bone bonding ability and biocompatibility with bone. The change in the calculated N4 value also indi-cate the conversion of both BO3 and BO4 strutural units associated with the formation of hydroxyapatite. Magnetic characteristics meas-ured and calculated through VSM measurements supporting the idea of using such material as a bioactive material that can be used in hyperthermia treatment.

Keywords: *Hyperthermia; Hench Bio-Glass; FTIR; XRD; Borate Glass.*

1. Introduction

Biomaterials based on metals and/or their alloys have been widely used as components for medical devices in orthopaedic surgeries including implants, plates, screws or as surgical devices as prosthetic devices of the human body. These products, together with high performance, can meet the requirements of biocompatibility, strong mechanical efficiency, low manufacturing costs and high corrosion resistance. [1]. Corrosion is the degradation mechanism that, due to the surface chemical contact of the substrate with its external atmosphere, transforms a material to alternative shape and structure [2].

The fight against HIV/AIDS and cancer care has been an important topic lately and as one of the millennium goals. Per year, millions of cases are reported, and millions of cancer-related deaths are also reported. The emergence of emerging technology is improving this situation, and new cancer therapy methods have been introduced in the clinical protocol including hyperthermia by using bioactive or biocompatible glasses or even their glass-ceramic derivatives [3]. Hyperthermia is a term employed to describe techniques of heat application to the tumour usually associated with an already well-established routes of treatment, especially radiotherapy and chemotherapy. Hyperthermia was first considered as a therapeutic therapy in 1970 [4]. Such route of treatment results in a destruction of malignant cells regardless of healthy one that not suffer any non-reversible damage [5]. This consequence is associated to the tumor hypoxic atmosphere, which result in an acidic media connected with the thermal treatment and to the consequent cytoplasmatic destruction.

Tumors are usually heated more quickly than normal surrounding tissues, since the blood vessels and nervous systems in the tumours are poorly formed, and cancer cells are readily damaged by heat therapy, since there is inadequate oxygen supply to the tumour from the blood vessels. Hyperthermia is an important method for treating cancers, since this heat therapy does not harm healthy body cells due to proper heat dissipation caused by normal blood flow [6]. The temperature of tumour cells can be increased by indirect heating provided by various magnetic materials in the range of 42-46 ^{0}C [5]. Magnetic materials exposed to a magnetic AC field can exhibit extraordinary heating effects associated with losses in the material reversal process during the magnetization process [7].

For this purpose a large number of ferri and ferromagnetic bioactive glass ceramics materials for magnetic induction hyperthermia have been developed. Magnetic materials that seeded locally within the treated organ can act as thermo motor that generate heat under the effect of AC magnetic fields [8]. These ferrimagnetic glass-ceramics are bioactive and biocompatible and therefore can form a layer of biologically active bone-like apatite on their surface. Moreover, when they are placed under an alternating magnetic field, they generally heat effectively cancer cells to be necrotized by magnetic hysteresis loss. Another important advantage, characteristic of glasses and glass-ceramics, is their ability to functionality, making them suitable for magnetic drug targeting [5]. The heating capacity depends on the material properties, such as magnetocrystalline anisotropy, magnetic properties, particles size, composition, frequency of alternating magnetic field and microstructure of the matrials [9].

Research in recent years has centred on the creation of new types of materials that induce the biochemical reaction of living tissues in order to achieve a tight chemical connection between the prothesis and the tissue through biological fixation[10]. The oldest bioactive substance is bioactive glass 45S5 (Bioglass ®), first mentioned by Hench et al[11].
Presented work aims to introduce a new type of glass modified with a magnetic partner (Co ions) and to study the structural changes associated with prolonged immersion times in simulated body fluids (SBF) or other corrosive solutions to be used as a suitable material for hyperthermia treatment.

2. Materials and methods

2.1. Materials

Pure chemical reagent of orthoboric acid as a source for B_2O_3, Ammonium dihydrogen phosphate as a source of P_2O_5 supplied by Sigma Aldrich Co. while sodium oxide and calcium oxide obtained from their carbonate partner supplied by ElNasr Pharmaceuticals. Cobalt oxide supplied by Riedel De Haen Co. All chemicals were used as received without further purification. Glass samples were prepared via traditional melt quenching route with a nominal composition $xCoO . (45-x)B_2O_3 . 24.5 Na_2O . 24.5 CaO . 6 P_2O_5$ wt% where x = 0, 0.2, 0.5, and 1.0 as shown in Table (1).

Table 1: Glass Nomination and Composition

Glass	B_2O_3	CoO	CaO	Na_2O	P_2O_5
Base	45.0	0.0	24.5	24.5	6
Co 0.2	44.8	0.2	24.5	24.5	6
Co 0.5	44.5	0.5	24.5	24.5	6
Co 1.0	44.0	1.0	24.5	24.5	6

2.2. Characterization and testing techniques

XRD experimental data measured for fine glassy powdered samples were accomplished to ensure the amorphous nature of studied samples and to check absence of phase separation or crystallization processes that were formed during the heat treatment of the analyzed samples. X-Ray diffraction was performed using a Brucker Axs-D8 setup (Metallurgical Institute, EL-Tebben-Helwan). A source Cu Kα radiation has been utilized (λCu Kα =0.154600 nm). Data was steeply accumulated with an intervals of 0.02º, using a time of 0.4 seconds over a 2θ diffraction angle range of 4 to 70°. The obtained spectra were compared to the complied standards using Joint Committee on Powder Diffraction and standards (JCDPS).
FTIR spectra of the studied glass were recorded at room temperature (25 ºC) in the spectral range (400-4000 cm^{-1}) and 2 cm^{-1} step resolution using a FTIR spectrometer (type Nicolet is10, ThermoFisher Co.). Measurements were applied on powder glassy samples dispersed in KBr, as a matrix material in ratio 1:100. The same weight of powder of each composition was taken. For complete analysis, the weighted mixtures were intended to a load of 5 ton/cm^2 to get disc like shape. The spectra of IR absorption were immediately performed to avoid moisture attack. The spectrum of each glass sample represent an average of separated scans, which was normalized to the spectrum. The evolution of the network connectivity was thus followed.
A quantitative analysis for the infrared spectrum has been analyzed and stimulated by Gaussian functions using the standard curve fitting [Peak Fit] program in which peak positions of each band intensities and widths have been varied automatically by the program to find the best fit. The program was designed to define hidden peaks using numerical iterative methods and suitable peak definitions including height, intensity, and full width at half maximum (FWHM) and other remind factors that control the quality of fitting process. The spectra of IR were corrected for the noises of the dark current and background using two-point base line correction before fitting. Many trials have been applied using multi band of components on the basis of minimization of the deviations between simulated and experimental spectrum.
In order to investigate the magnetic behavior of the studied glasses which based on Faraday's law of magnetic induction, we have measured the magnetization (M) dependent curves of the magnetic field (H) at different CeO2 concentration $0 \leq x \leq 50$ mol%. The magnetic measurements were performed using a LakeShore Vibrating Sample magnetometer (VSM 7403, Metallurgical Institute, El-Tebbeen-Helwan). The specimen was filled into a tube and then placed in an applied field parallel to the vibrating direction. The magnetic hysteresis (M-H) loop was observed in magnetic field range of (-20.000 - 20,000 G) at room temperature. The magnetization values were divided by the sample weight, to obtain the magnetic moment per gram or emu/g as magnetization unit. The parameters extracted from hysteresis loop which used to characterize the magnetic properties of the sample include saturation magnetization (Ms), Saturation remenance magnetization (Mrs), coercivity (Hc), squareness ratio (SQR) and switching field distribution (SFD).
Glass samples were thermally heat-treated through a two-step regime to obtain glass ceramic derivatives. The first step was (nucleation stage). At this step sufficient nuclei sites were formed by the slow heat treatment of the glass to the first temperature 450 ºC with holding time 4 h. This step followed by the second step at which glass was further heated to reach the second chosen crystal growth temperature at 650 ºC for 6 hours. The specimens were then left to cool inside the muffle to room temperature at a rate of 30 ºC/h to remove residuals of thermal stresses and prevent crashing of samples. Synthesized glasses were crushed in a porcelain mortar and sieved to obtain homogenous fine powder.

3. Results

3.1. XRD analysis

Figure 1(a-d) reveals X-ray diffraction (XRD) pattern of the studied glasses before and after heat treatment and conversion to their respective glass-ceramic derivatives (a and b). XRD analysis was also performed for the same samples after being immersion for a prolonged time intervals in a simulated body fluid (SBF) an example for such samples immersed for 2 and 4 weeks were given in Figures (c, d). Analysis of the spectra of suh modified borate glasses can be considered as an efficient tool to verify the formation of the mineral apatite phase. The XRD pattern of all glasses were compared with JCPDS card for hydroxyapatite file number 9–0432 [12].

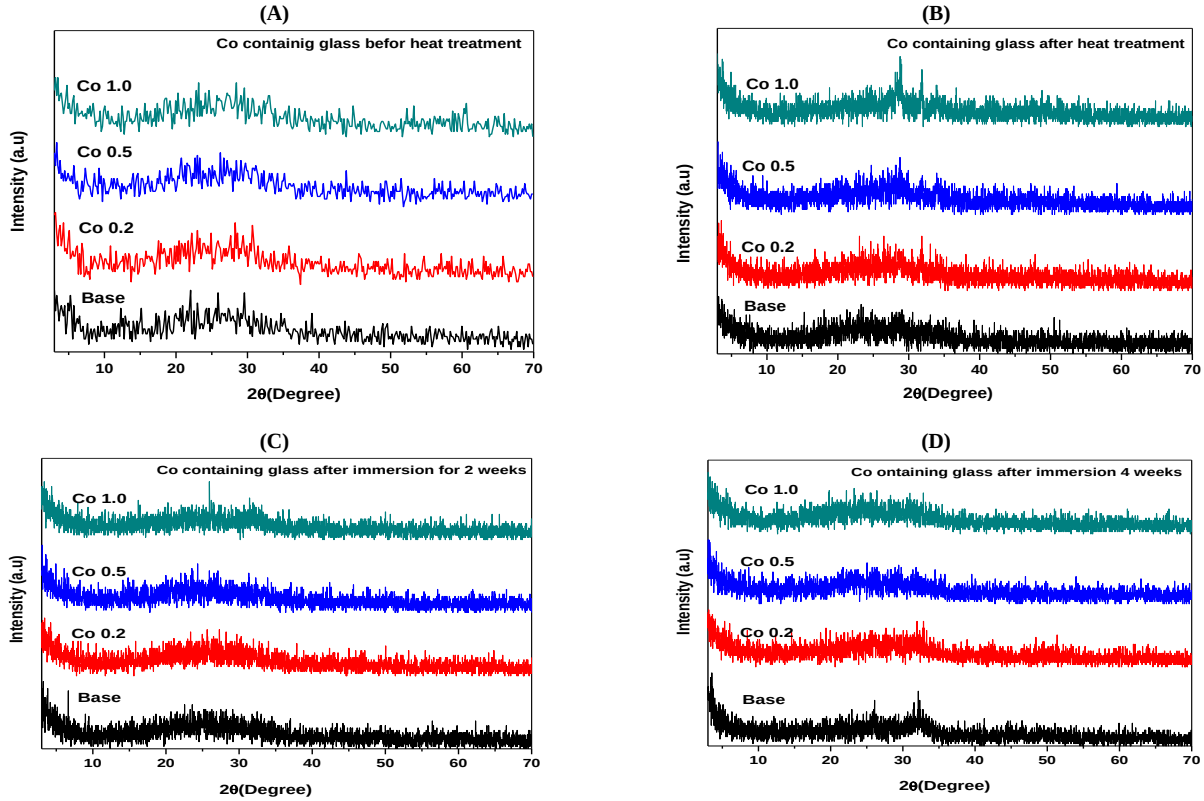

Fig. 1: XRD Pattern of Studied Glasses Before Heat Treatment (A), After Heat Treatment (B), After Immersion in SBF For 2 Weeks (C), and After Immersion in SBF for 4 Weeks (D).

3.2. Fourier transform infrared (FTIR)

Fourier transform infrared (FTIR) spectral data of glassy material can be used to identify structural groups within the matrix even if they are amorphous (glass) or containing crystalline phases (glass-ceramics). Therefore, FTIR absorption spectral data were measured for base glass and glasses that contain different amounts of dopant cobalt oxide before and after heat treatment (Figures (2.a, b)) to retrace the structural variations before and after adding cobalt oxide. It was clear that vibrational modes of both triangular and tetrahedral boron was observed at their respective wavenumber position previously reported by different authors [13-15] as reported in Table (2). The main differences is the resolving of superimposed peaks in the spectra of amorphous peaks into their respective separated peaks in the spectral data of heat treated samples.

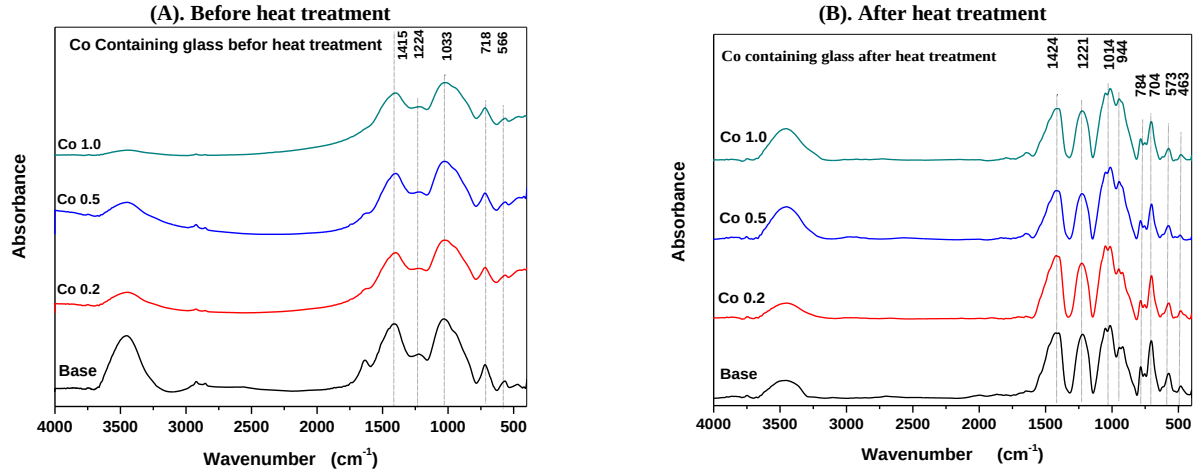

Fig. 2: (A), (B) FTIR Optical Absorption Spectra of Studied Samples Before and After Heat Treatment

Table 2: Peak Assignment of the FTIR Spectral Data of Studied Samples Before and After Heat Treatment

Wavenumber (cm^{-1})	Assignment
400-600	Cations region/ Modifier ions
600-800	Symmetrical bending vibrations of B-O-B (triangular units, BO_3)
800-1200	Symmetrical B-O stretching vibrations of tetrahedral borate units, BO_4+PO_4 such as tetra-borate and di-borate groups.
1200-1600	Asymmetrical stretching vibrations of triangular BO_3 borate unit, such as meta-borate chains, boroxol rings, pyro-borate and ortho-borate groups.
3457	This zone related to water and OH vibrations which indicate the hygroscopic nature of the modified glass.

Structural investigations were also performed for glasses that immersed in simulated body fluids for a prolonged time intervals (1, 2, 3, and 4 weeks) as indicated in figures (3(a-d). Figures (3.a-d) shows the structural variation of studied samples after different time intervals up to 4 weeks. It was clear that a distinct variation in the structural groups were observed from the first week due to the interaction between ions in the SBF and surface layer of borate bioactive glasses. it was noticed that no surface gel layer was formed in the surface of studied borate glass matrix due to the ease of solubility of such glasses.

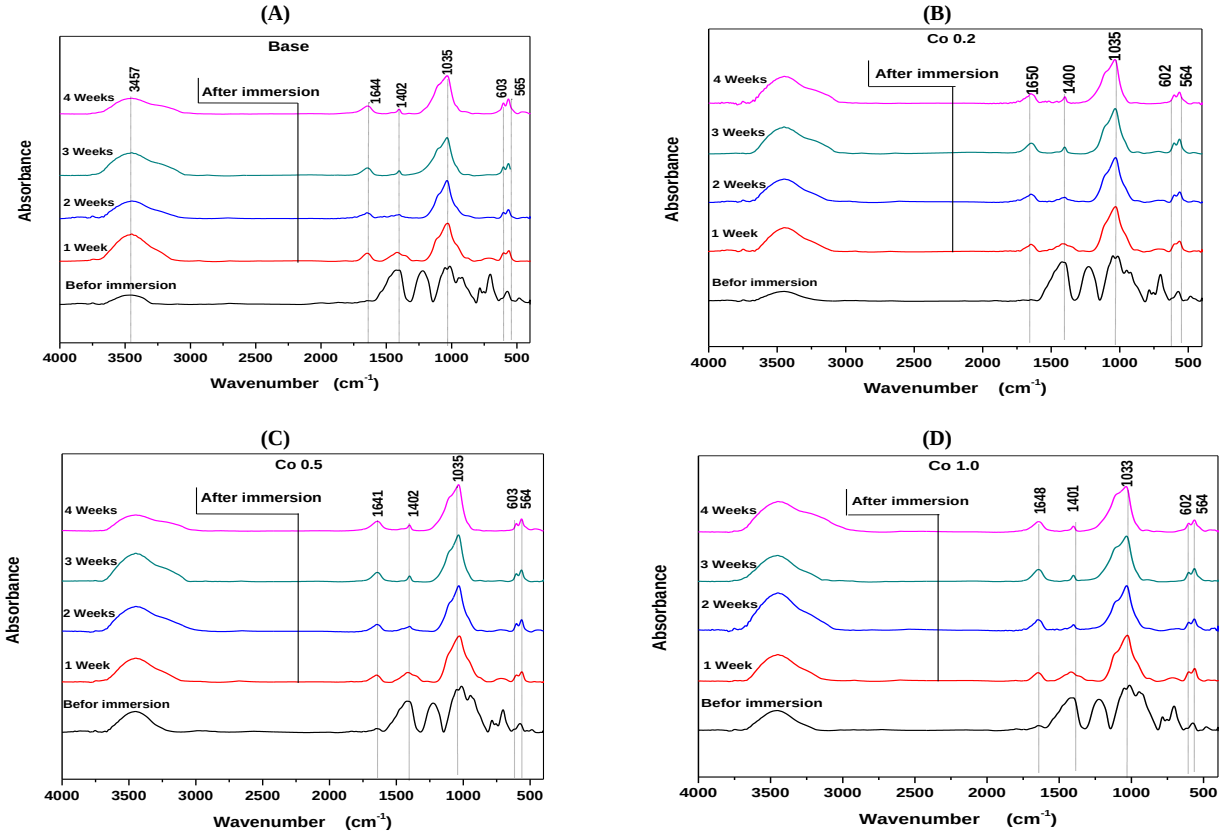

Fig. 3: (A-D) FTIR Optical Absorption Spectra of Studied Samples Before and After Immersion in SBF For Prolonged Times.

FTIR Spectral data for all measured samples can be truncated from 400-1800 cm^{-1} as they contain the main characteristic vibrational modes while the rest of spectra contains only OH vibrational mode represented by a broad peak originally located at about 3500-3600 m^{-1}. The remind spectra can be divided into three main regions. The first region characterize triangular borate units BO3 asymmetrical stretching modes vibrations of triangular including meta-borate, boroxol rings, pyro-borate and ortho-borates located between 1600-1200 cm^{-1}. The second region characterize tetrahedral borate units including tetra and di-borate units in combination with some other phosphate groups between 1200-800 m^{-1}. The last region located between 800-600 cm^{-1} characterize symmetric vibrations of triangular borate units [16].
All samples was deconveluoted to resolve all smearing bans that result from overlapping of both triangular and tetrahedral borate groups (BO3 and BO4). From such data the percentage of N4 coordination can be calculated and used to interpreted FTIR data in correlation with change in bridging and non-bridging oxygen's (BO and NBO) [17-19]. Figure (4.a, b) revels an exemplified deconvolution analysis of sample that contain higher concentration of Cobalt oxide (1 Wt%) employed to calculate the N4 variation with both heat treatment and immersion times. The N4 fraction can be calculated using the relative area corresponding to BO4 to that of both (BO3+BO4) from analyzed data. Figure (4) shows the variation of N4 with respect to the immersion times. It was observed that N4 increases with increasing the immersion time resulting from the conversion of BO3 and BO4 with a minor effect for the variation of Co concentration due to their lower content as indicated from Figure (5)

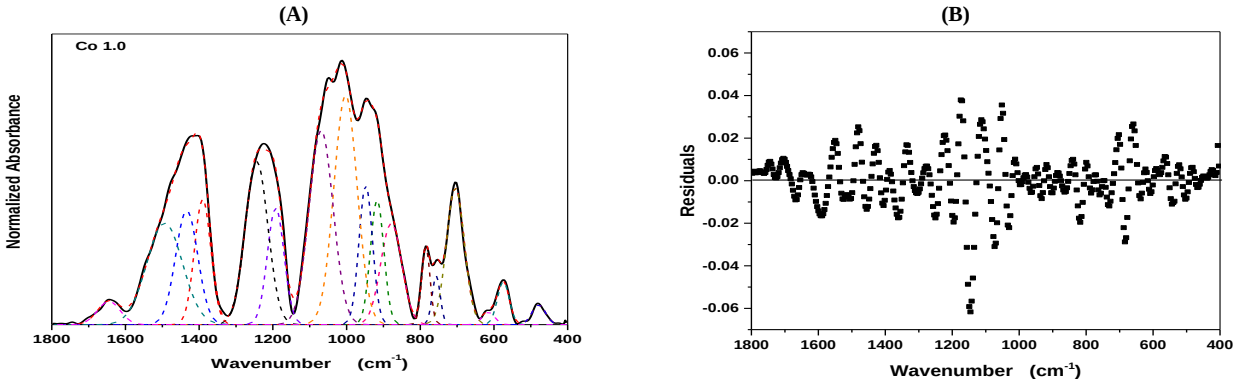

Fig. 4: (A), (B) an Exemplified Deconvolution Analysis of Sample That Contain Higher Concentration of Cobalt Oxide (1 wt%) Before Immersion in SBF.

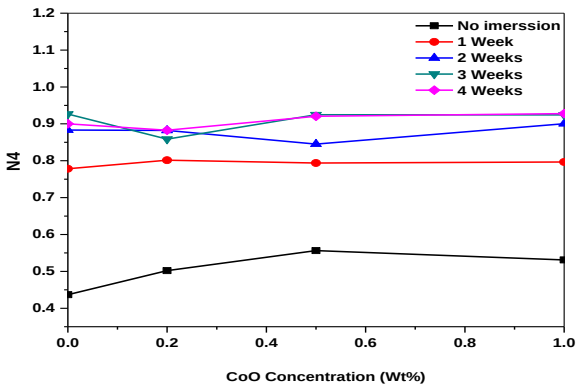

Fig. 5: Variation of the Four-Coordinated Boron as A Function of Cobalt Oxide Concentration and Immersion Times.

Vibrating sample magnetometer (VSM)

Figures (6.a, b) illustrate hysteresis loop of the studied sample containing dopant CoO 1wt% from which coercivity and squareness (ratio of residual magnetization to saturation magnetization) can be calculated for that sample before immersion in SBF and after 2 and 4 weeks immersion. The results that estimated and calculated from figure (6) were tabulated in Table (3) below. It was noted that magnetic characteristics of studied samples was strongly depend on the aspect ratio. The coercivity and the squareness increase drastically with the increasing aspect ratio, but their increase above aspect ratio 7 is rather limited. The reason for obtaining highest coercivity has been explained in terms of the increasing coercivity by the transition of ferromagnetic material from magnetic multi-domain to single-domain with change in particle size and the lowering coercivity of single-domain particles by the increasing contribution of the super-magnetism [16]. Ccomparison of all concentrations leads to the fact that the squareness is increased from 2 weeks to 4 weeks and reached to about 0.422 in the highest concentration.

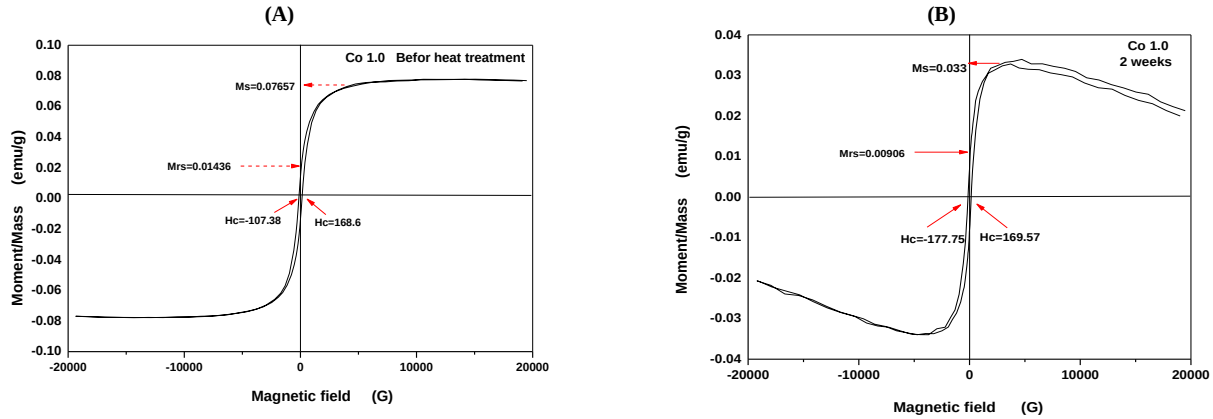

Fig. 6: (A-E) Illustrate Coercivity and Squareness (Ratio of Residual Magnetization to Saturation Magnetization) as A Function of Particle Volume of the Maghemite Particles with Different Aspect Ratios.

Table 3: Estimated and Calculated Magnetic Parameters of Glass-Ceramic Containing 1Wt% Coo Before and After Immersion in SBF

Sample	Immersion times	Saturation (Ms)	Remenance (Mrs)	Squareness (SQR)=Mrs/Ms	Coercivity +Hc	Coercivity -Hc	ΔH	SFD (ΔH/Hc)
Co 1.0	before	0.0766	0.01456	0.190	168.6	107.38	275.9	1.60
Co 1.0	2 Weeks	0.0330	0.00906	0.275	169.6	177.7	347.3	2.05
Co 1.0	4 Weeks	0.0268	0.01130	0.422	209.5	178.9	388.4	1.85

4. Discussion

Studied modified Hench Bioglass prepared through fully replacement of silica with boron oxide promote the advantage of ease solubility preventing formation of gel layer in addition to the ease of secretion of borate residuals through urine. Thus, syntheised glass preferred to be converted to their glass-ceramic derivative through a two-step crystallization process, nucleation and crystallization. X-ray diffraction analysis was used to approve the conversion of fully amorphous material to a material that contains at least one crystalline phase superimposed of th2e amorphous lattice. Such sharp bands were correlated with that reported for the hydroxyapatite previously studied by several authors. Structural variations and ability of bonding can be also retraced using both XRD and FTIR experimental data. FTIR absorption spectral data reveals presence of prominent peaks originally attributed to the presence of both trigonal and tetrahedral borate units labeled as BO3 and BO4 units. The splitting of the band originally located at 620 cm^{-1} can be assumed as an indication for the formation of hydroxyapatite combined with conversion of BO3 and BO4 units associated with a change in the four coordinated boron number N4 calculated using deconvolution analysis technique (DAT) previously reported elsewhere [20]. Variation of the N4 value indicate a strong ability for bone bonding through boron structural unit conversion. Magnetic properties of a slightly CoO-doped samples up to 1 wt% shows a great variation in magnetization process that can be interpreted in terms of single and multi-domain that lower coercivity supporting the idea of using such material during the thermal treatment of hyperthermia.

5. Conclusion

Samples of nominal composition xCoO . (45-x)B_2O_3 . 24.5 Na_2O . 24.5 CaO . 6 P_2O_5 wt% where x = 0, 0.2, 0.5, and 1.0 were successfully synthesized using traditionally melt quenching route. Corresponding glass-ceramics were also obtained through processes of nucleation and crystallization route at specific temperatures. The nature of amorphous glass structure was approved using XRD route. While, samples after crystallizations appears to contains a crystalline hydroxyapatite phase originally confirmed through comparison with the slandered diffraction pattern reported for hydroxyapatite. The same result was approved through observation of band splitting in the FTIR spectra especially after one week of immersion in SBF. The results were confirmed through calculation of the four coordinated boron number N4 that change dramatically after one week immersion. Obtained data shows also a little effect of CoO addition in the doping level. A distinct]changes in magnetic parameters with small addition of CoO suggesting use of such material for the treatment of hyperthermia.

References

[1] El-Rabiei MM, Bahrawy A, El-Feky HE, Negem, M, Safaa MM., Nady H (2020) The Effect of Ni Content on the Corrosion Resistance of Some Fe–Cr–Ni Alloys in Simulated Body Fluids in the Presence of H_2O_2 and Albumin. Journal of Bio-and Tribo-Corrosion 6(2):1-17. https://doi.org/10.1007/s40735-020-00350-1.

[2] Villanueva J, Trino L, Thomas J, Bijukumar D, Royhman D, Stack MM, Mathew MT (2017) Corrosion, tribology, and tribocorrosion research in biomedical implants: progressive trend in the published literature. Journal of Bio-and Tribo-Corrosion 3(1):1. https://doi.org/10.1007/s40735-016-0060-1.

[3] Aspasio RD, Borges R, Marchi J (2016) Biocompatible glasses for cancer treatment. In Biocompatible Glasses. Springer, Cham. (pp. 249-265). https://doi.org/10.1007/978-3-319-44249-5_10.

[4] Nielsen OS, Horsman M, Overgaard J (2001) A future for hyperthermia in cancer treatment?. European Journal of Cancer 37(13), 1587-1589. https://doi.org/10.1016/S0959-8049(01)00193-9.

[5] Bretcanu O, Verné E, Cöisson M, Tiberto PAOLA, Allia P(2006) Magnetic properties of the ferrimagnetic glass-ceramics for hyperthermia. Journal of magnetism and magnetic materials 305(2), 529-533https://doi.org/10.1016/j.jmmm.2006.02.264.

[6] Shah SA, Hashmi MU, Alam S, Shamim A (2010) Magnetic and bioactivity evaluation of ferrimagnetic $ZnFe_2O_4$ containing glass ceramics for the hyperthermia treatment of cancer. Journal of magnetism and magnetic materials 322(3), 375-381. https://doi.org/10.1016/j.jmmm.2009.09.063.

[7] Hergt R, Dutz S, Müller R, Zeisberger M (2006) Magnetic particle hyperthermia: nanoparticle magnetism and materials development for cancer therapy. Journal of Physics: Condensed Matter 18(38), S2919. https://doi.org/10.1088/0953-8984/18/38/S26.

[8] Baeza A, Arcos D, Vallet-Regí M (2013) Thermoseeds for interstitial magnetic hyperthermia: from bioceramics to nanoparticles. Journal of Physics: Condensed Matter 25(48), 484003. https://doi.org/10.1088/0953-8984/25/48/484003.

[9] Bahadur D, Giri J (2003) Biomaterials and magnetism. Sadhana, 28(3-4), 639-656. https://doi.org/10.1007/BF02706451.

[10] Abdelghany AM (2013) Novel method for early investigation of bioactivity in different borate bio-glasses. Spectrochimica Acta Part A: Molecular and Biomolecular Spectroscopy 100, 120-126. https://doi.org/10.1016/j.saa.2012.02.051.

[11] Hench LL, Splinter RJ, Allen WC, Greenlee TK (1971) Bonding mechanisms at the interface of ceramic prosthetic materials. Journal of biomedical materials research 5(6), 117-141. https://doi.org/10.1002/jbm.820050611.

[12] Alexopoulou, M., Mystiridou, E., Mouzakis, D., Zaoutsos, S., Fatouros, D. G., & Bouropoulos, N. (2016). Preparation, characterization and in vitro assessment of ibuprofen loaded calcium phosphate/gypsum bone cements. *Crystal Research and Technology*, *51*(1), 41-48. https://doi.org/10.1002/crat.201500143.

[13] Ouis MA, Abdelghany AM, ElBatal HA (2012) Corrosion mechanism and bioactivity of borate glasses analogue to Hench's bioglass. Processing and application of ceramics 6, 141–149. https://doi.org/10.2298/PAC1203141O.

[14] Abdelghany AM, Ouis MA, Azooz MA, ElBatal HA, El-Bassyouni GT (2016) Role of SrO on the bioactivity behavior of some ternary borate glasses and their glass ceramic derivatives. Spectrochim. Acta part A: Mol. Biomol. Spectrosc.152,126–133. https://doi.org/10.1016/j.saa.2015.07.072.

[15] Abo-Naf SM, Khalil EM, EL-Sayed EM, Zayed HA, Youness RA (2015) In vitro bioactivity evaluation, mechanical properties and microstructural characterization of Na_2O–CaO–B_2O_3–P_2O_5 glasses. Spectrochimica Acta Part A: Molecular and Biomolecular Spectroscopy 144, 88-98. https://doi.org/10.1016/j.saa.2015.02.076.

[16] Itoh H, Sugimoto T (2001) Synthesis of monodispersed magnetic particles by the gel-sol method and their magnetic properties. Studies in Surface Science and Catalysis 132, 251-254. https://doi.org/10.1016/S0167-2991(01)82080-2.

[17] Kamitsos, E. I., & Chryssikos, G. D. (1991). Borate glass structure by Raman and infrared spectroscopies. Journal of molecular structure, 247, 1-16. https://doi.org/10.1016/0022-2860(91)87058-P.

[18] Menazea, A. A., & Abdelghany, A. M. (2020). Gamma irradiated Hench's Bioglass and their derivatives Hench's Bioglass-ceramic for bone bonding efficiency. Radiation Physics and Chemistry, 108932. https://doi.org/10.1016/j.radphyschem.2020.108932.

[19] Okasha, A., Abdelghany, A. M., Wassel, A. R., & Menazea, A. A. (2020). Bone bonding augmentation and synergetic attitude of gamma-irradiated modified borate bioglass. Radiation Physics and Chemistry, 109018. https://doi.org/10.1016/j.radphyschem.2020.109018.

[20] Abdelghany, A. M. (2010). The elusory role of low level doping transition metals in lead silicate glasses. Silicon, 2(3), 179-184. https://doi.org/10.1007/s12633-010-9053-8.